Bio-optical properties of the Barents and Norwegian seas surface layer in summer 2017

Dmitry Glukhovets[1]

[1]Shirshov Institute of Oceanology, Russian Academy of Sciences

November 23, 2022

Abstract

A comparative study of the surface layer bio-optical properties of the Barents and Norwegian Seas in the summer of 2017 is carried out. Ship data were obtained during the 68th cruise of the R/V 'Akademik Mstislav Keldysh' (June-August 2017). Using a flow-through system, the fluorescence intensities of chlorophyll 'a' and dissolved organic matter, salinity and temperature of the water surface layer along the ship's route were continuously recorded. At the sampling stations, the reflectance spectra were measured. Samples were taken for spectral fluorescence and absorbance measurements performed with a laser spectrometer and an integrating cavity absorption meter. The results are compared with the data of direct determinations of the chlorophyll concentration. In the Barents Sea, the results of shipboard measurements are compared with the data of OLCI satellite scanner. Frequent continuous cloudiness prevented the use of ocean color data for the Norwegian Sea. A comparative study of the fluorescence, absorption, and reflectance spectra has shown the possibility of carrying out a rapid assessment of the phytoplankton species composition and its concentration. In particular, these data made it possible to detect the coccolithophore bloom in the Barents Sea. The change in the coefficients of the regression equation of chlorophyll fluorescence intensity and its concentration, determined by direct methods for different regions, is shown.

1

Bio-optical properties of the Barents and Norwegian seas surface layer in summer 2017

D. Glukhovets [a, b]

[a] *Shirshov Institute of Oceanology, Russian Academy of Sciences, Nakhimovskiy Prospekt, 36, Moscow, 117218*
[b] *Moscow Institute of Physics and Technology, Institutsky lane 9, Dolgoprudny, Moscow region, 141700*
e-mail: *glukhovets@ocean.ru*

Abstract
A comparative study of the surface layer bio-optical properties of the Barents and Norwegian Seas in the summer of 2017 is carried out. Ship data were obtained during the 68th cruise of the R/V 'Akademik Mstislav Keldysh' (June-August 2017). Using a flow-through system, the fluorescence intensities of chlorophyll 'a' and dissolved organic matter, salinity and temperature of the water surface layer along the ship's route were continuously recorded. At the sampling stations, the reflectance spectra were measured. Samples were taken for spectral fluorescence and absorbance measurements performed with a laser spectrometer and an integrating cavity absorption meter. The results are compared with the data of direct determinations of the chlorophyll concentration. In the Barents Sea, the results of shipboard measurements are compared with the data of OLCI satellite scanner. Frequent continuous cloudiness prevented the use of ocean color data for the Norwegian Sea. A comparative study of the fluorescence, absorption, and reflectance spectra has shown the possibility of carrying out a rapid assessment of the phytoplankton species composition and its concentration. In particular, these data made it possible to detect the coccolithophore bloom in the Barents Sea. The change in the coefficients of the regression equation of chlorophyll fluorescence intensity and its concentration, determined by direct methods for different regions, is shown.

Keywords: bio-optical properties, surface layer, CDOM, chlorophyll, fluorescence, Barents Sea, Norwegian Sea.

1. Introduction

The aim of this work is a comparative study of the bio-optical properties of the surface layer of the Norwegian and Barents seas waters by shipboard and satellite data. The effectiveness of such an integrated approach to the use of optical methods for studies of the Baltic, Norwegian and Barents Seas, according to data of 2014-2016 cruises, is shown in the work (Glukhovets et al., 2017).

The physical, optical and biological properties of the investigated seas are connected (Hancke et al., 2014). These properties are determined by the influx of salted and warm Atlantic waters from the southwest and less salted cold Arctic waters from the north (Loeng and Drinkwater, 2007). The border between these water masses in the Barents Sea is known as the Polar Front (Hancke et al., 2014; Oziel et al., 2015). Continuous measurements with the help of a flow-through system made it possible to separate these water masses to study their bio-optical properties.

2. Materials and methods
2.1. Research area

Shipboard data were collected during the 68th cruise of the R/V 'Akademik Mstislav Keldysh'. Underway measurements in Norwegian and Barents Seas were made from June 19 to August 16 2017. The route of expedition where measurements were taken is shown in Fig. 1. 69 ship stations (5516-5581 as several were repeated) were completed in the Norwegian and Barents Seas. The numbering is sequential; the numbers of some stations are shown on the map.

2.2. Data collection and processing

A flow-through system developed at the Ocean Optics Laboratory of the Shirshov Institute of Oceanology (Goldin et al., 2015) was used to conduct the shipboard measurements. It consists of a two-channel flow-through fluorimeter (FTF-2) with high-brightness LEDs and a thermosalinograph (Expert-002). The complex provides continuous measurements of the fluorescence intensities (I_{fl}) of the CDOM and chlorophyll 'a' (Chl 'a') in the near-surface layer along the ship's route, as well as the seawater salinity (S) and temperature (T).

In the FTF-2 the fluorescence intensity is measured at fixed spectral range, which includes the maxima of the fluorescence band. High-brightness LEDs (373 nm and 521 nm for CDOM and Chl 'a' channels respectively) working in a continuous mode, were used as sources of excitation in FTF-2. Photomultipliers were used to record fluorescence radiation. The emission detection ranges are formed with the help of coloured glass optical filters (transmittance maxima – 480 nm and 685 nm for CDOM and Chl 'a' channels respectively). The device provides measurements of I_{fl} in relative units. With the combination of excitation wavelength and registration, used in CDOM channel, the instrument measures the terrestrial humic-like DOC component fluorescence (Coble, 2007) mainly.

The water-intake system provides the instrument with seawater from 1-2 m depth. Due to the inconstancy of the lurch of the ship and rolling, relatively small variations in the depth of the water intake can occur. However, this does not affect the results of measurements, as on all sections of the route, except for relatively narrow frontal zones, the upper water meters are usually uniform: in work (Not et al., 2005) five meter sampling depths related to the mixed layer. In stormy weather conditions, there is an even greater mixing of the waters of the surface layer. The data-averaging interval was 15 s, which eliminates the effect of rolling and pitching. The relative error in I_{fl} measuring was <1%. The error in determining the salinity did not exceed 0.25 PSU, temperature – 0.12 °C. The calibration of the thermosalinograph was corrected on basis of the probe CTD measurements at the stations.

Fluorescence spectra of phytoplankton pigments and CDOM were measured on seawater samples using a two-channel laser spectrometer LS-2 and a LED spectrofluorometer LEDSF (excitation wavelengths – 401, 532 and 595 nm) developed at the Ocean Optics Laboratory of the Shirshov Institute of Oceanology.

Absorbance spectra $a(\lambda)$ were calculated according to the data of an ICAM (Integrating Cavity Absorption Meter) portable spectrophotometer developed at the Department of Biophysics of the Faculty of Biology of Moscow State University (Pogosyan et al., 2009) using method created at the Ocean Optics Laboratory of the Shirshov Institute of Oceanology (Glukhovets et al., 2018).

The ocean reflectance measurements were performed using a floating spectroradiometer (Artemiev et al., 2000).

Determination of chlorophyll concentration was performed by the spectrophotometric method (Jeffrey and Humphrey, 1975).

Chlorophyll concentration (Chl) defined by the semi-analytical OC4Me and Neural Network Case2R algorithms as well as coloured detrital and dissolved material absorption coefficient $a_{dg}(443)$ were used in this work. These data were received from Ocean and Land Colour Instrument (OLCI) ocean-colour scanner. The OLCI L2 satellite data were retrieved from the EUMETSAT website (https://codarep.eumetsat.int). Values for the comparison with shipboard data were made by averaging the L2 data over a grid with 3 x 3 pixel bins. Reduction of resolution can eliminate the effects that arise close to the clouds. All satellite data processing performed in the Matlab software package.

The data of INTERIM reanalysis (Dee et al., 2011) were used to show the total cloudiness and estimate the surface wind effects.

The National Ice Center's Interactive Multisensor Snow and Ice Mapping System (IMS) daily data at 4 km resolution (https://nsidc.org/data/G02156) were used to show the sea ice distribution.

3. Results and Discussion

Figure 2 shows the spatial distributions of the temperature, salinity, and fluorescence intensities of CDOM and Chl 'a' in the water surface layer obtained with the help of a flow-through measuring complex. The gaps correspond to the areas on which the work was temporarily stopped because of stormy weather. The results of the measurements show that the Norwegian Sea is affected by warm (T = 8-10 °C) salty (S > 35 psu) Atlantic waters carried by the Norwegian current. Further, the waters of this current penetrate the Barents Sea, where they mix with cold (T = 0-4 °C) Arctic waters with a lower salinity (S < 34.5 psu) coming from the north. Based on the results obtained with the help of a flow-through measuring complex, the position of the boundary between these water masses – the Polar Front – was found. According to the results (Parsons et al., 1996) the boundary of the Polar Front is an isotherm of 3-4 degrees. On the distributions of T and S (Fig. 2), Atlantic waters correspond to warm tones, the Arctic – to cold ones. On August 1 and August 12 2017 the route was crossed in the Polar Front area (74 °N, 34 °E). The coincidence of the values of T, S, I_{fl} CDOM and Chl 'a' at this point indicates the relative stability of the boundary position between Atlantic and Arctic waters in this period.

The spatial distribution of CDOM and Chl 'a' fluorescence intensities can become additional factors in the separation of water types. In general, the Arctic waters are characterized by a decreased intensity of chlorophyll fluorescence (Figure 2, bottom right), which coincides with the results of direct determinations of the Chl concentration. In the central part of the Barents Sea, the increased values of I_{fl} CDOM were registered. The fluorescence intensity measured at 480 nm increased from 1.0-1.1 r.u. up to 1.2-1.3 r.u. (Figure 2, lower left). The values of the gelbstoff absorption $a_g(400)$ at stations 5521, 5528 and 5542 (Fig. 1) did not exceed 0.05 m^{-1}, while at station 5581 $a_g(400)$ = 0.077 m^{-1}. That increase may emerge due to coccolithophore blooms, the presence of which is confirmed by the results of laboratory determinations. In the summer of 2017, coccolithophore blooms were recorded along the southern side of the Polar Front, which corresponds to the results of the works (Burenkov et al., 2011; Hovland et al., 2013; Signorini and McClain, 2009).

We cannot but pay attention to the feature of the section of the transect made near Franz Josef Land (all measurements made north of 78 °N and east of 40 °E). Here there is a positive correlation between S and I_{fl} CDOM (Pearson correlation coefficient is 0.83). A similar type of connection was recorded earlier in the bays of Novaya Zemlya (Glukhovets and Goldin, 2018). It was the consequence of glacial meltwater influence, which is fresh and contains less amount of CDOM (Drozdova et al., 2017). The area of the glaciers of Franz Josef Land is 12.7 thousand square kilometers, which is comparable with the area of glaciers of Novaya Zemlya – 22.1 thousand square kilometers (Moholdt et al., 2012). The melting rate of these glaciers has recently increased (Zheng et al., 2018). This process brings to an inflow of significant amount of desalinated water in the surface layer. The maps of the sea ice spatial distribution based on sea ice IMS data for July 5 (the month before the ship measurements) and on August 5 (the time when the ship measurements were made) showed a significant reduction in the sea ice area near Franz Josef Land during this period. Thus, ship data were obtained during the glaciers of the archipelago and sea ice active thawing. Sea ice contains less amount of CDOM than seawater: during sea ice formation in the adjacent Kara Sea CDOM rejection is about 50-70 % (Amon, 2003). All this means that the positive correlation between the S and I_{fl} CDOM near Franz Josef Land is caused by the influence of thawed waters – archipelago glacial and sea ice.

Measurements of the CDOM and phytoplankton pigments fluorescence spectra were performed at 59 stations. Fluorescence intensity spectra were obtained using the wavelengths of the exciting radiation 401, 532 and 595 nm. Peaks at wavelengths of 472, 650 and 741 nm, respectively, are due to Raman scattering; the maxima at a wavelength of 682 nm are due to the Chl 'a' fluorescence. For excitation of 401 nm wavelength, the Chl 'a' fluorescence peak is overlapped with a broad CDOM fluorescence band, whose maximum is close to 500 nm. The spectra are normalized to the intensity of the Raman scattering by the corresponding excitation wavelength and are given in the so-called Raman units (RU). All measured fluorescence spectra

for the surface horizon (5 m) are shown in Figure 3 (blue lines correspond to the Barents Sea, green ones – Norwegian). Shapes of fluorescence spectra obtained in the surface layer of the seas under study are similar to each other. The amplitudes of the Chl 'a' fluorescence peaks vary in the same range.

The fluorescence excitation, with each of the wavelengths used, has its advantages. The blue range is well absorbed by both CDOM and Chl 'a', but just the effect of the CDOM band on the Raman band can affect the results of normalizing the fluorescence intensity of Chl 'a' to the intensity of the Raman scattering in a negative way. The green channel is convenient for studying the fluorescence of Chl 'a' because of the closeness of its fluorescence band to the Raman scattering peak, but it is poorly suited for the study of additional pigments, in particular phycocyanin of cyanobacteria. The orange channel has the greatest sensitivity, and is best suited for the study of cyanobacteria either.

The peak amplitude of chlorophyll fluorescence indicates the productivity of water. However, the I_{fl} Chl 'a' is related to its concentration ambiguously. This relationship depends on the phytoplankton species composition and the algae adaptation to external conditions (Karabashev, 1990). In the studied areas, four regions were identified, where the linear relationship of the fluorescence intensity of Chl 'a' with its concentration ($C_{Chl} = A*I_{fl}$) is characterized by high values of determination coefficient ($R^2 > 0.92$). These regions are shown with dashed lines in Fig. 1. Figure 4 shows scattering diagrams for an excitation wavelength of 401 nm. To increase the sample size we used the data obtained at all the horizons of these stations. Differences in the slopes of the regression lines should be taken into account when performing an absolute calibration of fluorimeters.

The greatest coefficient of the regression equation between I_{fl} Chl 'a' and its concentration ($A = 4.7$) was obtained in the Barents Sea in (Fig. 2). That means that for a given concentration of Chl, the fluorescence intensity of Chl in this region is smaller than in other regions. During the shipboard measurements in this part of the Barents Sea, the sky was free of clouds. Stations 5578-5581 were performed during the daytime. The decrease of I_{fl} in the area of coccolithophore bloom can be due to mechanism of non-photochemical quenching (Voronova et al., 2009), emerging from increased light intensity in sunny weather.

Reflectance $\rho(\lambda)$ and absorbance $a(\lambda)$ spectra for stations from the selected regions are shown in Fig. 5. Station 5581 is made in the area of coccolithophore blooms. Coccolithophore cells and coccoliths significantly increase the scattering and almost do not influence absorption. Because of this, the reflectance spectral values at station 5581 are twice as high as those obtained at other stations. The high values of $\rho(\lambda)$ and the common values of $a(\lambda)$ made it possible to operatively identify that the coccolithophores were the dominant phytoplankton type in this region.

The increased content of CDOM in the bloom area (Fig. 2) determines increase in $a(\lambda)$ and an a decrease in $\rho(\lambda)$ in the short-wavelength region. Spectra for stations from 1 to 3 regions are similar to each other. The reflectance spectrum obtained at station 5521 is slightly different: it has a rise in the short-wave region. This feature may be explained by the smaller content of CDOM in the western part of the Norwegian Sea (Fig. 2).

Due to frequent and dense cloudiness over the investigated areas in summer 2017 the quantity of available ocean colour satellite data at the required quality was very limited. Besides that, an important requirement for satellite data is the minimum possible time difference with shipboard measurements. Based on these requirements, several OLCI images were found. The most indicative of them relates to the coccolithophore bloom in the Barents Sea. The OLCI data closest in time (August 14 at 9 AM GMT) to those of the expedition were selected for the analysis. Figure 6 shows the spatial distribution of chlorophyll concentration according to OC4Me standard algorithm. Continuous ship measurements in this region were carried out on August 14-15 (the route is shown in Fig. 6 with a black line).

According to satellite data in the bloom region, the Chl concentration can reach 3 mg/m^3, while according to the results of direct determinations, the concentration of Chl in this area did not exceed 1.75 mg / m^3 (station 5580). The mentioned above increased content of CDOM in the

coccolithophore bloom area (Figure 2, lower left; station 5581 in Fig. 5) may be one of the reasons of sharp increase in Chl (Kopelevich et al, 2004). The standard semi-analytical OC4Me algorithm assumes additional CDOM absorption by chlorophyll and overestimates it. The Neural Network Case2R algorithm gives even greater Chl concentration values (up to 6 mg/m^3).

It should be noted that a good qualitative agreement of the position of the bloom boundaries was recorded with the help of a flow-through measuring system: an increase in CDOM and Chl 'a' fluorescence intensities in the region of 70.5 °N and 35 °E (Fig. 2). However, the values of coefficient of determination of the results of shipboard fluorescence measurements and satellite data is relatively small: $R^2 = 0.60$ for the OC4Me algorithm and $R^2 = 0.33$ for the Neural Network Case2R algorithm. Perhaps, this is the result of the daily mobility of the bloom boundaries caused by the water circulation and near-surface wind taken place during the ship measurements.

4. Conclusions

A comparative study of bio-optical properties of the Barents and Norwegian seas surface layer in summer 2017 is performed. Continuous distributions of seawater temperature, salinity, CDOM and Chl 'a' fluorescence intensities allowed to find the position of the Polar Front. The fluorescence spectra obtained in the surface layer of the seas under study are similar in shape and vary in the same range in amplitude of Chl fluorescence peak.

Previously, in the work by (Glukhovets and Goldin, 2018), a positive correlation of CDOM fluorescence intensity and salinity in the Kara Sea bays near the melting glaciers of Novaya Zemlya was recorded. In this paper, a similar type of relationship, associated with the effect of glacial and sea ice meltwater, at the transect performed near Franz Josef Land is recorded.

Four regions (two in the Barents Sea and Norwegian Sea), where the strong linear relationships of the fluorescence intensity of Chl 'a' with its concentration were registered, have been identified. Their regression equation coefficients varied from 2.7 to 4.7. The greatest coefficient was obtained in the coccolithophore bloom area in the Barents Sea. It may be explained by the mechanism of non-photochemical quenching.

In the coccolithophore bloom area in the Barents Sea, satellite and shipboard measurements are in good qualitative agreement. OLCI algorithms overestimate the values of Chl concentration, while the OC4Me output is closer to the results of direct Chl determinations than The Neural Network Case2R algorithm.

Studies based on data obtained in June-August 2017 showed that the Barents and Norwegian seas are interesting and dynamic regions, the bio-optical properties of which are influenced by various factors. Trends, related to climate change, will be manifested there most clearly. That determines the importance of future studies to understand the seasonal and interannual variability of the bio-optical properties of the Barents and Norwegian seas surface layer.

References:

1. Amon R.M.W. The role of dissolved organic matter for the organic carbon cycle in the Arctic Ocean. In: Stein, R., MacDonald, R. (Eds.), The Organic Carbon Cycle in the Arctic Ocean. Springer, Berlin, pp. 83-99 (2003).
2. Artemiev V.A., Burenkov V.I., Vortman M.I., Grigoriev A.V., Kopelevich O.V., Khrapko A.N. Sea-truth measurements of ocean color: a new floating spectroradiometer and its metrology. Oceanology. 40(1):139-45 (2000).
3. Burenkov V.I., Kopelevich O.V., Rat'kova T.N., Sheberstov S.V. Satellite observations of the coccolithophorid bloom in the Barents Sea. Oceanology. 51(5):766 (2011).
4. Coble P.G. Marine optical biogeochemistry: the chemistry of ocean color. Chemical reviews, 107(2), pp.402-418 (2007).
5. Dee D.P., Uppala S.M., Simmons A.J., Berrisford P., Poli P., Kobayashi S., Andrae U., Balmaseda M.A., Balsamo G., Bauer D.P., Bechtold P. The ERA-Interim reanalysis: Configuration and performance of the data assimilation system. Quarterly Journal of the royal meteorological society. 137(656):553-97 (2011).
6. Drozdova A.N., Patsaeva S.V., Khundzhua D.A. Fluorescence of dissolved organic matter as a marker for distribution of desalinated waters in the Kara Sea and bays of Novaya Zemlya archipelago, Oceanology, 57(1), 41-47 (2017).
7. Glukhovets D.I., Goldin Yu.A. Surface layer desalination of the bays on the east coast of Novaya Zemlya identified by shipboard and satellite data. Oceanologia. 2018 Jul 17. (in print)
8. Glukhovets D.I., Kopelevich O.V., Sahling I.V., Artemiev V.A., Pautova L.A., Lange E.K., Kravchishina M.D. Biooptical characteristics of the surface layer of the Baltic, Norwegian, and Barents seas in summer 2014–2016 from shipboard and satellite data. Oceanology. 57(3):410-8 (2017).
9. Glukhovets D.I., Sheberstov S.V., Kopelevich O.V., Zaytseva A.F., Pogosyan S.I. Measuring the sea water absorption factor using integrating sphere. Light & Engineering. 26(1) (2018).
10. Goldin Yu.A., Shatravin A.V., Levchenko V.A., Ventskut Y.I., Gureev B.A., Kopelevich O.V. Analysis of spatial variability of f luorescent intensity of seawater in western part of the Black Sea, Fundam. Prikl. Gidrofiz, 7(1), 11-20 (2015).
11. Hancke K., Hovland E.K., Volent Z., Pettersen R., Johnsen G., Moline M., Sakshaug E. Optical properties of CDOM across the Polar Front in the Barents Sea: Origin, distribution and significance. Journal of Marine Systems. 130:219-27 (2014).
12. Hovland E.K., Dierssen H.M., Ferreira A.S., Johnsen G. Dynamics regulating major trends in Barents Sea temperatures and subsequent effect on remotely sensed particulate inorganic carbon. Marine Ecology Progress Series. 484:17-32 (2013).
13. Jeffrey S.T., Humphrey G.F. New spectrophotometric equations for determining chlorophylls a, b, c1 and c2 in higher plants, algae and natural phytoplankton. Biochemie und physiologie der pflanzen. 167(2):191-4 (1975).
14. Karabashev G.S., 1990. Fluorescence in the ocean (Doctoral dissertation, Monterey Institute of International Studies). (1990).
15. Kopelevich O.V., Burenkov V.I., Ershova S.V., Sheberstov S.V., Evdoshenko M.A. Application of SeaWiFS data for studying variability of bio-optical characteristics in the Barents, Black and Caspian Seas. Deep Sea Research Part II: Topical Studies in Oceanography. 51(10-11):1063-91 (2004).
16. Loeng H., Drinkwater K. An overview of the ecosystems of the Barents and Norwegian Seas and their response to climate variability. Deep Sea Research Part II: Topical Studies in Oceanography. 54(23-26):2478-500 (2007).
17. Moholdt G., Wouters B., Gardner A. S. Recent mass changes of glaciers in the Russian High Arctic. Geophysical Research Letters, 39(10) (2012).

18. Not F., Massana R., Latasa M., Marie D., Colson C., Eikrem W., Pedrós-Alió C., Vaulot D., Simon N. Late summer community composition and abundance of photosynthetic picoeukaryotes in Norwegian and Barents Seas. Limnology and Oceanography, 50(5), pp.1677-1686 (2005).
19. Oziel L., Sirven J., Gascard J.C. The Barents Sea polar front and water masses variability (1980-2011). Ocean Science Discussions, 12(2) (2015).
20. Parsons A.R., Bourke R.H., Muench R.D., Chiu C.S., Lynch J.F., Miller J.H., Plueddemann A.J., Pawlowicz, R. The Barents Sea polar front in summer. Journal of Geophysical Research: Oceans, 101(C6), pp.14201-14221 (1996).
21. Pawlowicz R. M_Map: A mapping package for Matlab. University of British Columbia Earth and Ocean Sciences. [Online]. Available: https://www.eoas.ubc.ca/~rich/map.html. (2000).
22. Pogosyan S.I., Durgaryan A.M., Konyukhov I.V., Chivkunova O.B., Merzlyak M.N. Absorption spectroscopy of microalgae, cyanobacteria, and dissolved organic matter: Measurements in an integrating sphere cavity. Oceanology. 49(6):866-71 (2009).
23. Schlitzer R. Ocean Data View, odv.awi.de (2017).
24. Signorini S.R., McClain C.R. Environmental factors controlling the Barents Sea spring-summer phytoplankton blooms. Geophysical Research Letters. 36(10) (2009).
25. Voronova E.N., Konyukhov I.V., Kazimirko Y.V., Pogosyan S.I., Rubin A.B. Changes in the condition of photosynthetic apparatus of a diatom alga Thallassiosira weisflogii during photoadaptation and photodamage. Russian journal of plant physiology. 56(6):753 (2009).
26. Zheng W., Pritchard M. E., Willis M. J., Tepes P., Gourmelen N., Benham T. J., Dowdeswell J. A. Accelerating glacier mass loss on Franz Josef Land, Russian Arctic. Remote Sensing of Environment, 211, 357-375 (2018).
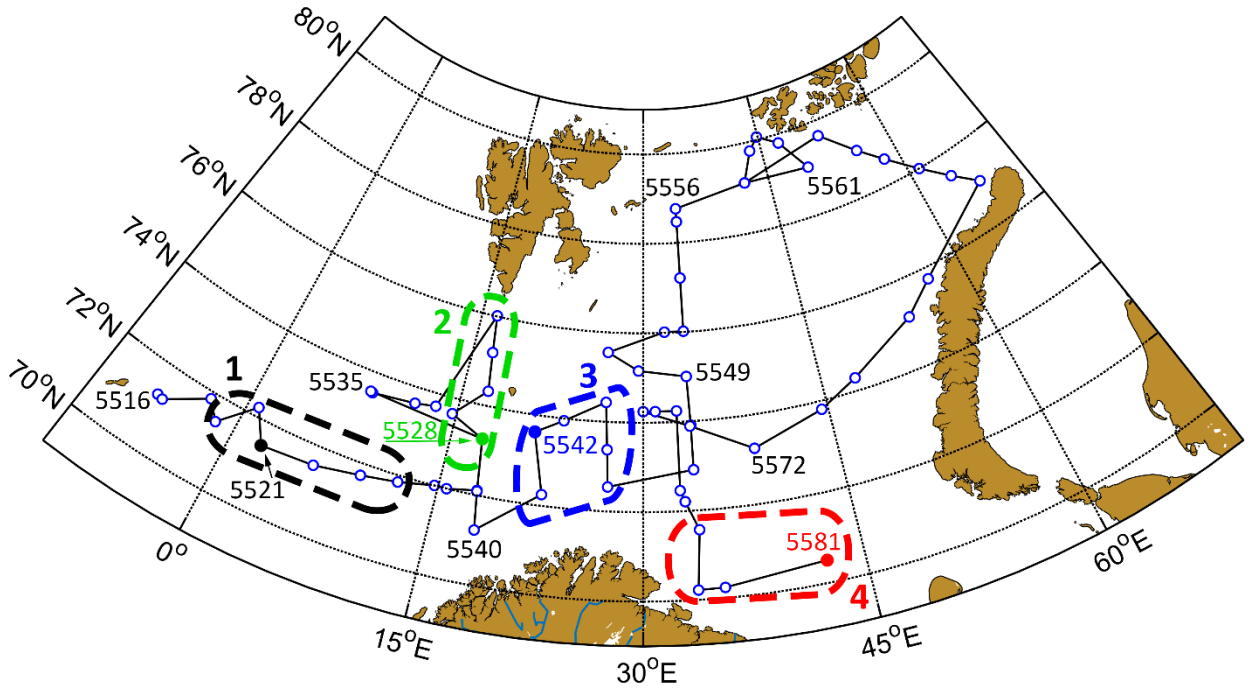
Figures:

Fig. 1. Route of 68th cruise of R/V Akademik Mstislav Keldysh in Barents and Norwegian seas (June 19 – August 16, 2017). Blue circles indicate cruise stations, coloured points – stations shown in Fig. 5, numbered dashed frames – regions for Fig. 4. The m_map package for MATLAB was used to prepare the figure (Pawlowicz, 2000).
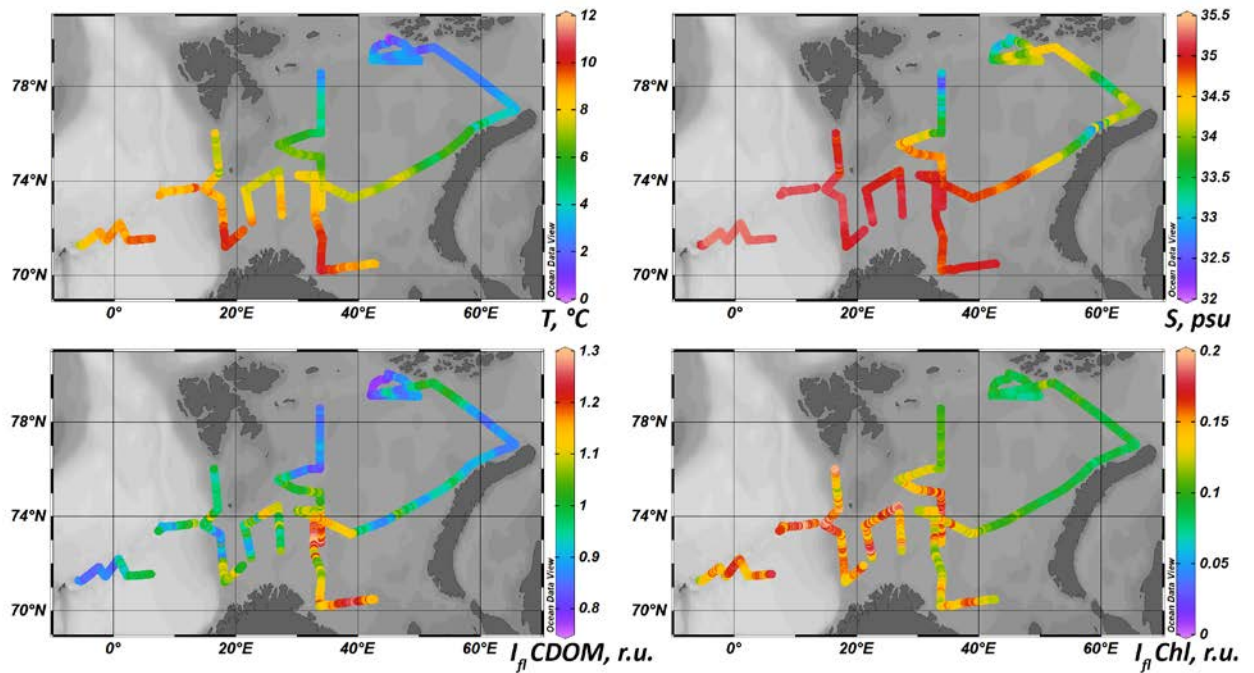

Fig. 2. Spatial distributions of temperature (top left), salinity (upper right) and fluorescence intensities of the CDOM (lower left) and Chl 'a' (bottom right) in the water surface layer. Both fluorescence intensities are given in relative units. July 19 - August 16, 2017. The figure was drawn using ODV (Schlitzer, 2017).
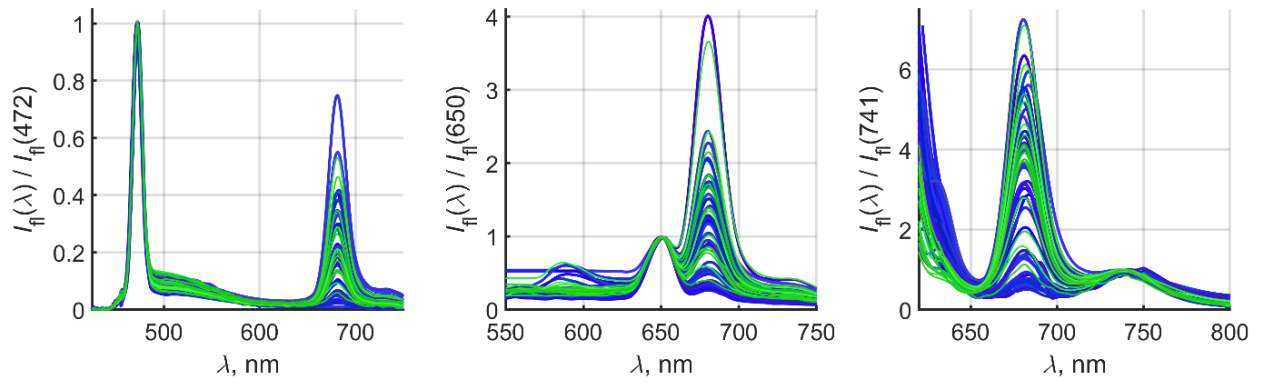
Fig. 3. Fluorescence spectra of surface horizons samples, normalized to the signal intensity at the Raman scattering wavelength. Excitation 401 nm (left), 532 nm (center) and 595 nm (right). Blue lines correspond to the Barents Sea (43 stations), green – Norwegian ones (16 stations).
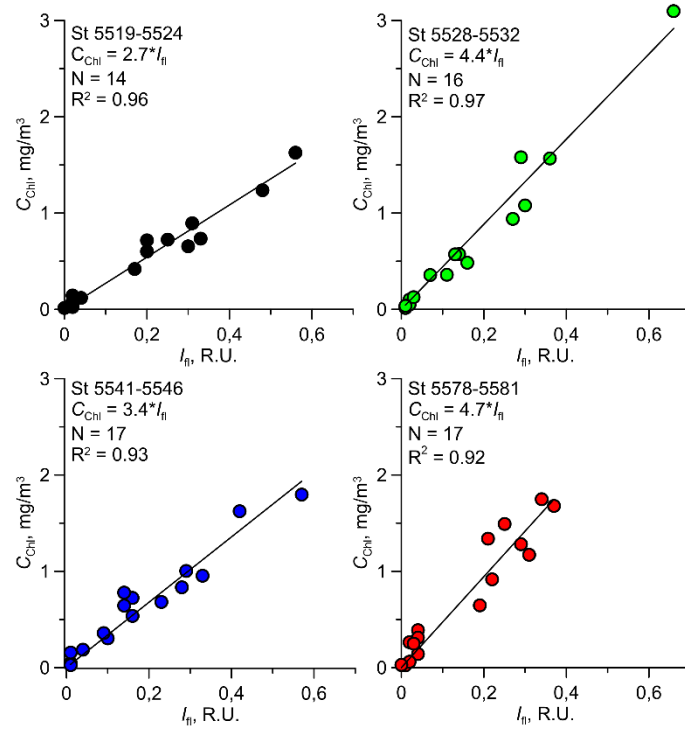

Fig. 4. Scattering diagrams of chlorophyll 'a' fluorescence intensity and its concentration for all stations inside selected regions shown in Fig. 1. Excitation wavelength is 401 nm.
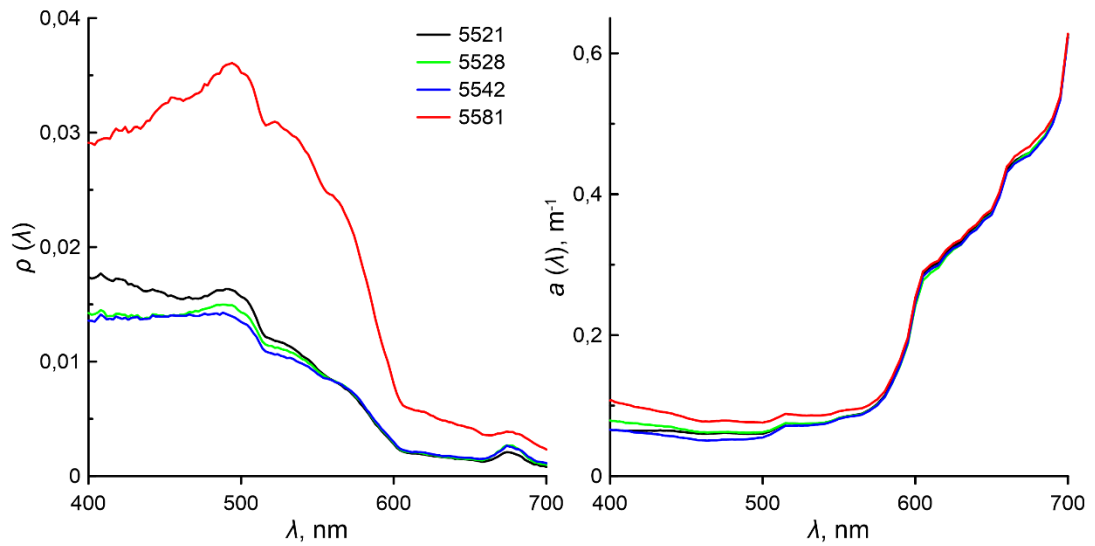
Fig. 5. Reflectance (left) and absorbance (right) spectra for stations of regions shown in Fig. 1.
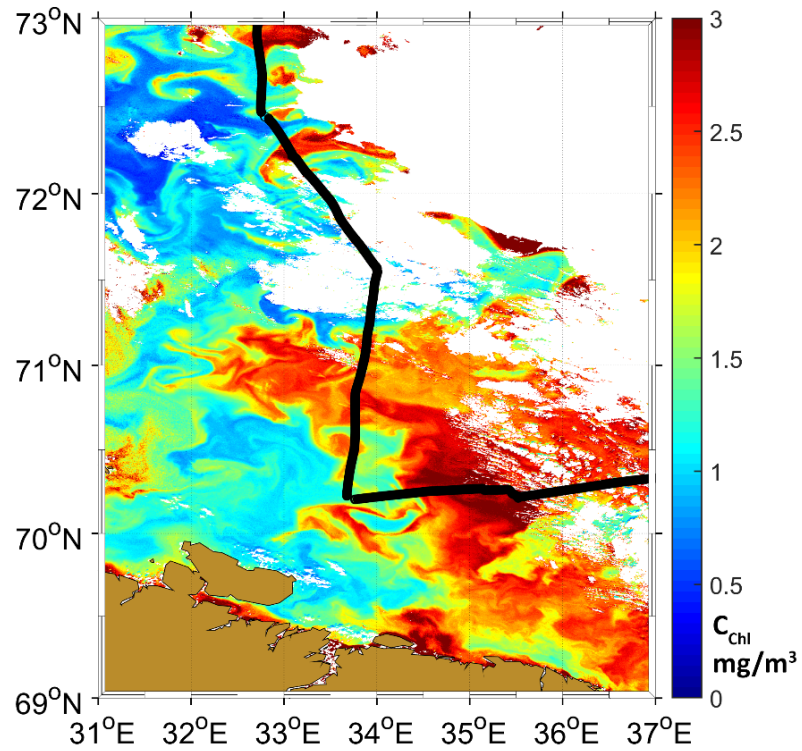

Fig. 6. Spatial distribution of chlorophyll 'a' concentration according to OLCI data (OC4Me algorithm) and the corresponding part of the route. The m_map package for MATLAB was used to prepare the figure (Pawlowicz, 2000).